

# Dynamical States, Stochastic Resonance and Ratchet Effect in a Biharmonically Driven Sinusoidal Potential

W.L. Reenbohn and Mangal C. Mahato\*

*Department of Physics, North-Eastern Hill University, Shillong-793022, India*

(Dated: March 3, 2022)

## Abstract

Two stable dynamical states of trajectories of an underdamped particle, under appropriate conditions, appear naturally in a sinusoidal potential when driven by a low amplitude biharmonic external field. These states are quite stable at low temperatures but make transitions between them as the temperature is raised. The proper choice of the biharmonic drive makes it possible for the system to show, at the same time, *both* the phenomena of stochastic resonance and ratchet effect. Ratchet effect, in this case, a consequence of the biharmonic drive, is obtained over a large domain of parameter space. However, stochastic resonance can be obtained only over a restricted (sub)domain of parameter space and owes its existence largely to the existence of the two dynamical states.

PACS numbers: : 05.10.Gg, 05.40.-a, 05.40.jc, 05.60.Cd

---

\*Electronic address: mangal@nehu.ac.in

## I. INTRODUCTION

The phenomenon of stochastic resonance (SR) was discovered[1] almost a decade prior to some innovative experiments[2] that brought the ratchet effect (RE) to renewed attention. SR is a phenomenon that shows a maximum in the response of a nonlinear system to a weak (subthreshold) input signal of a given frequency as the strength of noise in the input signal (or in the system) is varied. There has been intense investigations on the subject both theoretically and experimentally and have been reviewed extensively[3, 4]. However, the developments have been confined mostly to *bistable systems*; some of the early examples include the model Landau potential (theory), Schmitt trigger circuit, two-mode ring lasers (experiment), etc[5–7]. In sharp contrast, RE is a phenomenon in which a net current is obtained in *periodic potential systems* without application of any apparent bias, albeit, again in the presence of noise or zero-mean fluctuating forces. The subject of study (RE) since had a phenomenal growth[8–10]. Both the phenomena were hailed as important scientific developments with harmonious consequences[11].

In the beginning of the current resurgence of investigations RE was put forth as an important model to explain material transport along microtubules in biological systems. There are essentially two prominent models of RE; other models can be considered as variants of these two but are important on their own right. In one of the two models (rocked ratchet) the mean slope of the periodic potential is changed continuously (or abruptly) between positive and negative values[12]. This is the model we are interested in this work. In the other important model (of flashing ratchets) an asymmetric periodic potential of fixed strength is switched on and off either randomly or periodically[13]. Based on the latter model, RE was soon demonstrated experimentally in a colloidal particle system[14]. Both the phenomena (SR and RE), however, are counterintuitive and operate under nonequilibrium conditions in presence of noise.

In order for both the phenomena of SR and RE to occur in the same system, a driven periodic potential system needs to exhibit SR. As mentioned earlier the study of SR is largely confined to bistable or two-well systems. The occurrence of SR in periodic potential systems has not been conclusively proved analytically. However, some recent numerical investigations unmistakably indicate existence of SR in underdamped periodic potential systems too[15, 16]. This opens up the possibility of seeking both the phenomena to occur in

the same system under the same conditions. The present work shows that the simultaneous occurrence of SR and (rocked) RE is a distinct possibility even in case of underdamped symmetric periodic potential systems. It has been found earlier that SR and RE occur simultaneously in an overdamped flashing ratchet where the periodic potential is considered asymmetric[17]. As far as the present authors are aware that is the only report where RE and SR are genuinely found to occur simultaneously and the two phenomena are shown to have a close relation.

In that work[17], the power spectrum of the cosine of the position  $x(t)$  for all  $t \geq 0$  gives a dominant peak at the potential switching frequency at non-zero temperatures. This peak shows a maximum at a temperature very close to where the ratchet current has the largest value. Since the maximum of the power spectrum peak shows SR it was concluded that there is a close connection between SR and RE. Curiously, at zero temperature the power spectrum shows strong peaks at frequencies about one third (and multiples thereof) of the potential switching frequency. These intra-(potential)well breathings seem unrelated to switching field and disappear as the temperature is raised. In contrast, in the present work the frequency of external field is necessarily taken to be close to the natural frequency of oscillation at the bottom of the potential wells. Also, we do not really find any strong evidence of a close relationship between the two phenomena.

Periodic potentials are almost ubiquitous and stochastic motion of particles along periodic potentials have been studied extensively[18]. The examples include, crystals, semiconductor heterostructures, RCSJ model of Josephson junctions, microtubules, etc. Therefore, the occurrence of optimised signal (SR) and material transport (RE) together seems a very attractive possible proposition and needs to be investigated.

It has been shown earlier[15, 16] that when an underdamped particle, subjected to temporally periodic (sinusoidal) field, moves in a spatially periodic (sinusoidal) potential, the trajectory  $x(t)$  of the particle shows periodic behavior at low temperatures. The amplitude of  $x(t)$  and its phase relationship with the external field  $F(t)$  depend on the amplitude and frequency of  $F(t)$ , the friction coefficient  $\gamma$  and also on the initial conditions of position  $x(0)$  and velocity  $v(0)$ . A small range of frequencies ( $\omega = \frac{2\pi}{\tau}$ ) of  $F(t)$  close to the natural frequency ( $\omega_0 = 1$ ) of free oscillation at the bottom of the sinusoidal potential have a remarkable influence on the nature of trajectories.

In a narrow range around  $\tau = 2\pi$  of the period  $\tau$  of  $F(t)$  two distinct kinds of trajectories

$x(t)$  are realized: one having a small phase lag  $\phi$  with respect to  $F(t)$  and the other with a rather large  $\phi$  and amplitude. These two trajectories  $x(t)$  genuinely have the status of dynamical states having distinct basins of attraction in the  $(x(0) - v(0))$  phase space. A particle in the in-phase (small  $\phi$ ) state usually dissipates on the average much less energy per period,

$$\overline{W} = \int x(t)dF(t)$$

than in the out-of-phase (large  $\phi$ ) state. For a given value of  $\tau$  and the friction coefficient  $\gamma$  the relative abundance of the states in the  $(x(0),v(0)=0)$  space over a period of the potential  $V(x)$  (for example,  $[-\frac{\pi}{2} \leq x(0) < \frac{3\pi}{2}]$  for  $V(x) = -\sin(x)$ ) and also their relative stability depend on the amplitude  $F_0$  of  $F(t)$ . For a given set of  $\tau$ ,  $\gamma$ , and  $F_0$ , as the temperature is gradually increased, the relative abundance of the two dynamical states also change on the average and conspire together in such a way that the overall average energy dissipation  $\langle \overline{W} \rangle$  shows a maximum. In the periodic potential systems  $\langle \overline{W} \rangle$  is preferable and appropriate as a quantifier of SR over the signal to noise ratio[19]. Thus it is shown that SR is obtained in a periodic potential system but is explained in terms of transitions between the two dynamical states just as in the case of bistable systems. It may, however, be noted that in the conventional SR in double-well potential systems transition between the two states takes place at frequencies close to the Kramers rate of passages between the two wells. The frequencies of the drive field  $F(t)$  in the bistable systems, therefore, turn out to be about a factor of  $10^{-2}$  of the frequencies used in the present study. In the present work we consider a biharmonic external field  $F(t)$  with the main component of frequency  $\omega$  close to  $\omega_0$  and an additional component either of frequency  $2\omega$  (harmonic) or  $\omega/2$  (subharmonic).

As in the case of pure sinusoidal drive (described above), when the underdamped particle in the sinusoidal potential is driven by a biharmonic (harmonic or subharmonic) field similar dynamical states are realized. However, now the states become more complex and richer. As an illustration, the  $\overline{W}$  calculated over a period  $\tau$ , for  $\gamma = .12$ ,  $\tau = 8.0$ , the fraction of the main frequency term ( $f_m = .2$ ) ( $f_m$  is defined in the next section), and temperature  $T = .000001$ , are plotted as a function of  $F_0$ , the amplitude of the main frequency component of the drive in Fig.1. (All the parameters are given in dimensionless units, as described in the next section.) For convenience (and also to avoid the difficulty of assigning unambiguously the value of phase lag  $\phi$ ), we name the dynamical states (based on the amplitude of trajectories) as small-amplitude (SA) or large-amplitude (LA) states instead of in-phase

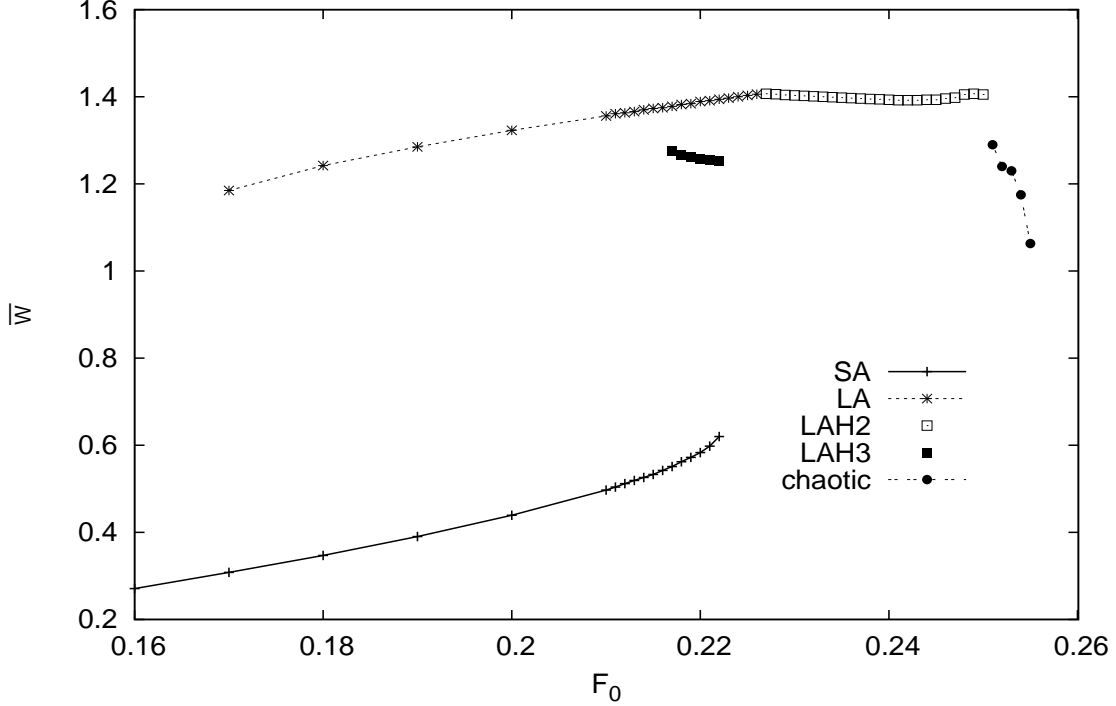


FIG. 1: The figure shows the input energies  $\overline{W}$  of various dynamical states SA, LA, LAH2, LAH3 and chaotic, occurring when driven by a biharmonic drive of amplitude  $F_0$ ,  $f_m = 0.2$ , the period of the main frequency component  $\tau = 8.0$  at  $T = 0.000001$ .

and out-of-phase states.

As is indicated in Fig.1, we obtain three kinds of LA states in the harmonic drive case: LA (with period  $\tau$ ), LAH2 (with period  $2\tau$ ) and LAH3 (with period  $3\tau$ ). These LA states are obtained in different regimes of  $F_0$  and have different  $\overline{W}$ . If the value of  $F_0$  is increased beyond 0.25, the trajectories no longer remain periodic but become chaotic even at as low a temperature as .000001. The representative trajectories, along with their stroboscopic plots, corresponding to these states are shown in Fig.2.

The relative stability and hence the relative abundance of these states existing at a given temperature decide the value of  $\langle \overline{W} \rangle$  at that temperature[16]. The maximum shown by  $\langle \overline{W} \rangle$  as a function of temperature indicates the occurrence of SR. However, the significance of such a peak, as a signature of SR, loses its meaning if it happens to occur at a temperature comparable to or higher than the potential barrier height itself. On the other hand, there could be situations, for example at large amplitudes of  $F_0$ , where  $\langle \overline{W} \rangle$  may

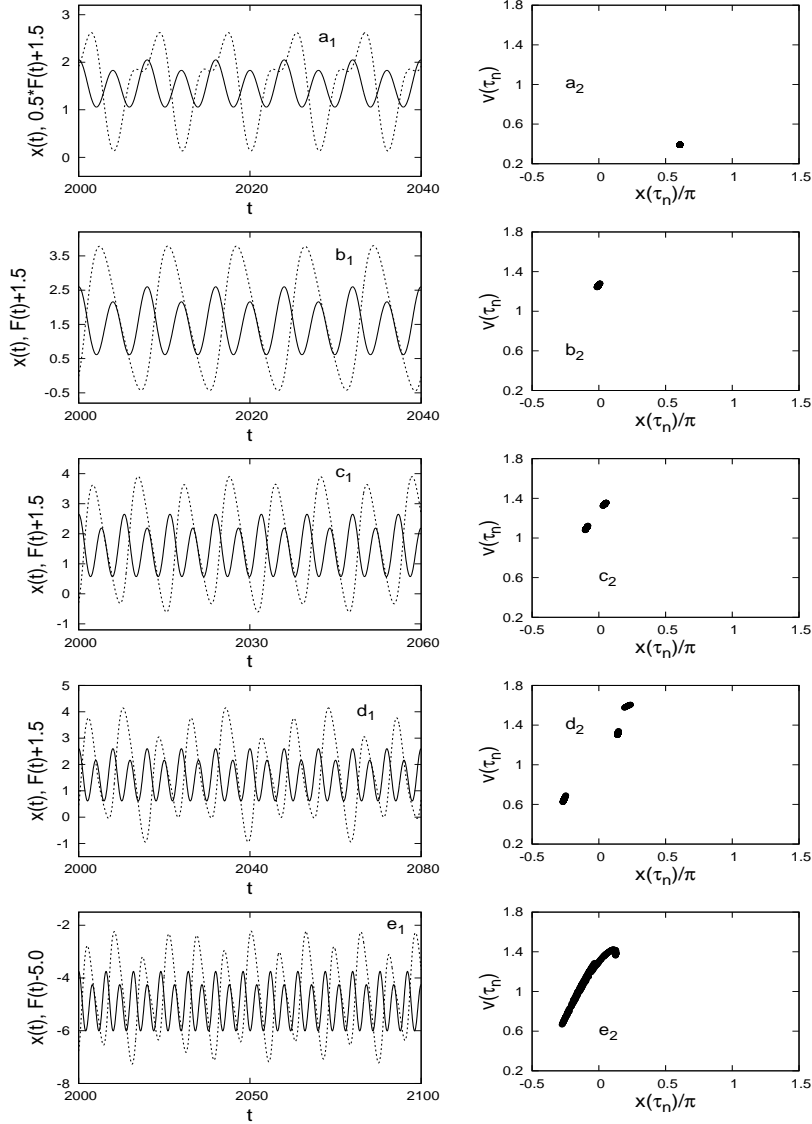


FIG. 2: The particle trajectories (dotted lines) of states SA, LA, LAH2, LAH3 and chaotic states of Fig.1. For comparison the field  $F(t)$  are also plotted (continuous line) along with the trajectories. The corresponding stroboscopic plots are also shown on the adjacent panel as Figs. 2  $a_2$ ,  $b_2$ ,  $c_2$ ,  $d_2$  and  $e_2$  at  $t = \tau_n = n\tau$ ,  $n = 0, 1, 2, \dots$ .

peak sharply at such low temperatures that only intra-(potential)well transitions between states take place. These peaks cannot be considered as an indication of occurrence of SR in a periodic potential. These restrictions make the domain of occurrence of SR in the parameter space quite narrow. However, RE has a comparatively large domain of occurrence.

From Fig.1, we find that there is a range of  $F_0$  where the two states LA and SA coexist in the harmonic drive case. This is the range of  $F_0$  where SR is found to occur. As the

amplitude is increased, the states LAH3 also appear and one can also see peaking of  $\langle \overline{W} \rangle$  with temperature. However, this peaking of  $\langle \overline{W} \rangle$  cannot be genuinely ascribed to SR because it takes place at a low temperature with only intra-well transitions between the states. Thus, we find that SR is due to transitions between the states SA and LA even in this case of biharmonic drive and the dynamical states LAH3 and LAH2 do not contribute to SR.

In the next section, the mathematical model will be discussed. The biharmonic drive parameters will be clarified. In Sec.3 the numerical method adopted and results obtained will be described in detail. Finally, in Sec.4 the results obtained will be discussed and conclusions of the work will be given.

## II. THE MODEL

As usual, the motion of an underdamped particle of mass  $m$  moving along the one dimensional spacing  $x$  in a sinusoidal potential  $V(x)$  and driven by a time periodic forcing  $F(t)$  subjected to a Gaussian thermal fluctuating force  $\xi(t)$  of mean zero is given by the Langevin equation[18]

$$m \frac{d^2x}{dt^2} = -\gamma \frac{dx}{dt} - \frac{\partial V(x)}{\partial x} + F(t) + \sqrt{\gamma T} \xi(t). \quad (2.1)$$

Here,  $\gamma$  is the coefficient of frictional force experienced by the particle while in motion with velocity  $\frac{dx}{dt}$  and is related to the fluctuating force through the fluctuation-dissipation theorem

$$\langle \xi(t) \xi(t') \rangle = 2\delta(t - t'). \quad (2.2)$$

Here  $T$  is the temperature (in energy units,  $k_B = 1$ ) of the heat bath with which the particle is in thermal contact. The potential is taken as

$$V(x) = -V_0 \sin(kx), \quad (2.3)$$

and the external periodic force is considered biharmonic in nature

$$F(t) = F'_0 (f_m \cos(\omega t) + f_h \cos(2\omega t + \theta)) \quad (2.4)$$

in case of harmonic field, and

$$F(t) = F'_0 (f_m \cos(\omega t) + f_h \cos(\frac{\omega}{2}t + \theta)) \quad (2.5)$$

in case of subharmonic field. Here,  $f_m$  is the fraction of the main frequency ( $\omega$ ) term and  $f_h (= 1 - f_m)$  is the fraction of the harmonic (subharmonic) frequency term.  $F(t)$  can be rewritten, for example, as

$$F(t) = F_0(\cos(\omega t) + \alpha \cos(2\omega t + \theta)), \quad (2.6)$$

where

$$F_0 = F'_0 f_m, \quad (2.7)$$

and the ratio

$$\alpha = \frac{f_h}{f_m}. \quad (2.8)$$

For simplicity and convenience the equations are rewritten in dimensionless units by setting  $m = 1$ ,  $V_0 = 1$ ,  $k = 1$ , with reduced variables denoted again now by the same symbols. Thus, the Langevin equation takes the form

$$\frac{d^2x}{dt^2} = -\gamma \frac{dx}{dt} - \frac{\partial V(x)}{\partial x} + F(t) + \sqrt{\gamma T} \xi(t), \quad (2.9)$$

where the reduced potential  $V(x) = -\sin(x)$ . We define the effective potential

$$U(x, t) = V(x) - xF(t), \quad (2.10)$$

with  $F(t)$  given, for example, by the equation of the same form

$$F(t) = F_0(\cos(\omega t) + \alpha \cos(2\omega t + \theta)), \quad (2.11)$$

for the harmonic drive, and

$$F(t) = F_0(\cos(\omega t) + \alpha \cos(0.5\omega t + \theta)), \quad (2.12)$$

for the subharmonic drive, but with the new dimensionless  $F_0$  equal in magnitude to the fraction  $\frac{F_0}{V_0 k}$  of the old dimensioned quantities and similarly for  $\omega$  and  $t$ , leaving, of course, the magnitude of  $\omega t$  same, etc[20]. Notice that, in this dimensionless form, the natural frequency  $\omega_0$  of oscillation at the bottom of any well of the potential equals 1, as mentioned in the Introduction. Therefore, so long as  $\gamma \ll 1$  we are working in the underdamped case. We keep the period  $\tau$  of  $F(t)$  of the main frequency term such that  $\omega (= \frac{2\pi}{\tau}) \approx \omega_0$  appropriate for the study of SR in the sinusoidal potential.



Note that whatever be the values of the parameters  $F_0$ ,  $\alpha$ ,  $\theta$ , the total impulse applied on the particle over a period

$$I = \int F(t)dt \quad (2.13)$$

is zero. For  $\theta = 0$  and  $\pi$ , for example, large forces are applied over a smaller period in one direction but small forces act over a longer period in the other direction. This kind of force profiles are known to result in ratchet effect[9]. Certain organisms, analogously, use power (swift) and reverse (slower) strokes of their flagella to aid locomotion.  $\theta = \pi$  gives the same  $\langle \overline{W} \rangle$  as  $\theta = 0$ , that is the same SR profile. Both  $\theta$  values will show RE but they will result in opposite net current directions. In contrast to  $\theta = 0$  and  $\pi$ , for  $\theta = \frac{\pi}{2}$ ,  $F(t)$  has a profile like an asymmetric saw-tooth repeated periodically. Here same kind of forces act in both directions but the increasing and decreasing slopes of  $F(t)$  are different. Such  $F(t)$  profiles also are known to exhibit ratchet effect[9, 10]. In all cases friction plays an important role and so does the noise.

The detailed numerical solution of the Langevin equation and analysis thereof, as described in the following, brings out the essential features of SR and RE in the system resulting from the biharmonic drive.

### III. NUMERICAL RESULTS

We solve the Langevin equation, Eqn.(2.2), numerically to obtain the position  $x(t)$  of the particle as time  $t$  progresses. The second-order Heun's method is suitably adapted[21] to solve the Langevin equation (2.2) as an initial value problem for the purpose. We choose integration-time-step size  $\Delta t = 0.001$ . We take the initial velocity  $v(0) \equiv v(t = 0) = 0$  for all cases. The initial position  $x(0) \equiv x(t = 0)$  are chosen at 100 equispaced points  $x_i$ ,  $i = 1, 2, \dots, 100$  between the two consecutive peaks, e.g.,  $[0 \leq x_i < 2\pi]$ . The input energy, or work done by the field on the system (or equivalently energy dissipated by the system to the environment),  $W$ , in a period  $\tau$  of the external field  $F(t)$ , is calculated as[22]:

$$\begin{aligned} W(t_0, t_0 + \tau) &= \int_{t_0}^{t_0 + \tau} \frac{\partial U(x(t), t)}{\partial t} dt, \\ &= - \int_{t_0}^{t_0 + \tau} x \frac{\partial F}{\partial t} dt \\ &= - \int_{F(t_0)}^{F(t_0 + \tau)} x dF. \end{aligned} \quad (3.1)$$

Therefore,

$$W(t_0, t_0 + \tau) = - \oint x dF = A, \quad (3.2)$$

where  $A$  is the magnitude of the area of the hysteresis loop  $x(F)$ . The average input energy per period,  $\overline{W}$ , averaged over an entire trajectory spanning  $N_1$  periods of  $F(t)$ , is

$$\overline{W} = \frac{1}{N_1} \sum_{n=0}^{n=N_1} W(n\tau, (n+1)\tau) = \overline{A}, \quad (3.3)$$

where  $\overline{A}$  is the area of the mean hysteresis loop  $\overline{x}(F)$ . In our calculation, typically, we solve Eqn. (2.2) for  $N_1 = 10^5$  periods of  $F(t)$  for each initial condition  $x(0)$  and take an ensemble average over all initial conditions to obtain  $\overline{x}(t)$  and  $\langle \overline{W} \rangle$ . The ratchet current or the mean velocity  $\overline{v}$  is calculated by dividing the mean distance travelled by the total run time.

Before we proceed to investigate the effect of biharmonic field on the occurrence of SR and RE it will be quite educative to see the effect of the frequency  $\omega$  ( $= 2\pi/\tau$ ) of the pure sinusoidal drive. As has been indicated earlier, a pure sinusoidal drive cannot yield RE in a symmetric sinusoidal potential system. We, therefore, study the occurrence of the two dynamical states LA and SA which are responsible for SR and find the domain in the parameter space of  $(\gamma - \tau)$  where LA and SA occur simultaneously.

### A. Pure sinusoidal drive

We restrict our study to the amplitude  $F_0 = 0.2$  of the external field  $F(t) = F_0 \cos(\omega t)$  at  $T = .000001$  for the occurrence of the states LA and SA. Note that, in the pure sinusoidal drive case, we set  $f_m = 1$ . As mentioned earlier, we determine the nature of states (LA or SA) by looking at the particle trajectories for 100 uniformly distributed initial positions  $x(0)$  drawn from inside of one period of the sinusoidal potential.

Fig. 3 shows the diagram of existence of LA and SA states in the  $(\gamma - \tau)$  plane. For a given  $\gamma$  we find only LA state for small  $\tau$  values. As  $\tau$  is increased at a certain value of  $\tau$  SA too begins appearing. This  $\tau$  sets the boundary between regions of existence of pure LA states and the simultaneous occurrence of both SA and LA states. On further increase of  $\tau$  the fraction of LA states decreases (and concurrently the fraction of SA states increases) and at a certain value of  $\tau$  the fraction of LA states becomes zero for the first time. This value of  $\tau$  sets the boundary between region of existence of the pure SA states and the

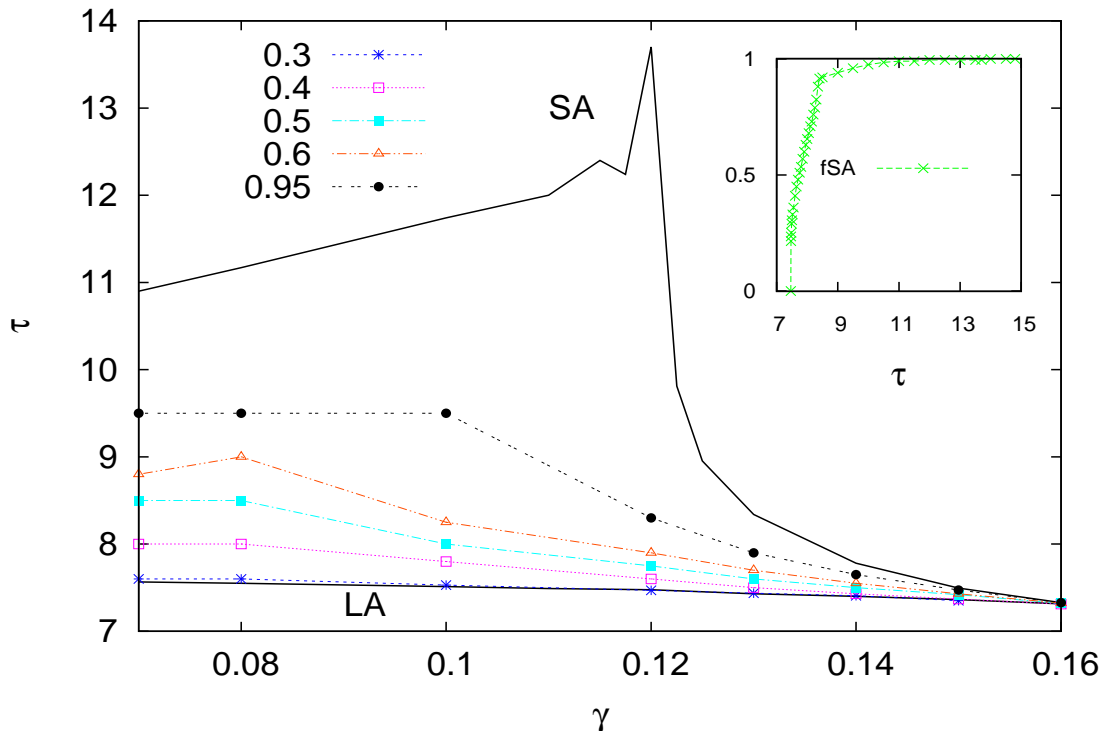


FIG. 3: The loci in the  $\tau - \gamma$  plane of the fractions (fSA= 0, 0.3, 0.4, 0.5, 0.6, 0.95, and 1.0) of SA states in the coexistence region of the states SA and LA when the system is driven by a sinusoidal field of period  $\tau$  and amplitude  $F_0 = 0.2$  in a medium of uniform friction  $\gamma$ . The inset shows the variation of fSA as  $\tau$  is varied for  $\gamma = 0.12$ . It shows a large discontinuous jump of 0.215 (from 0) at  $\tau = 7.466$  and a very gradual and slow approach to fSA=1 at large  $\tau$  values.

region of coexisting states of LA and SA. Together with these extreme boundary lines of fractions 0 and 1 of the SA states are also plotted the loci of fractions .3, .4, .5, .6, and .95 of SA. As can be seen from the figure there is a large space between the locus of fraction .95 of SA and the boundary where LA disappears. This is because for certain small number of initial positions  $x(0)$  the LA states continue to exist even for large values of  $\tau$ . This is particularly noticeable around  $\gamma = .12$ . However, as explained below, the states appearing in this subspace do not make any significant impact on our study of SR.

In the inset of Fig. 3 are plotted the fractions (fSA) of states SA as  $\tau$  is varied. The inset shows that the appearance of SA is very rapid and 100 percent LA boundary stays close to  $\tau = 7.5$ . However, the disappearance of LA is very slow and gradual and LA (together with SA) continues till a value of  $\tau$  as large as 14. It also shows that there is a small range

of  $\tau$ , close to  $\tau = 7.5$ , where both the states exist in significant fractions. As will be clear in the following this remark has important bearing on SR for the biharmonic drive. Now, as the temperature (noise strength) is increased from this small value transitions take place between the states SA and LA. Consequently, the average input energy  $\langle \overline{W} \rangle$  changes as the temperature is varied.

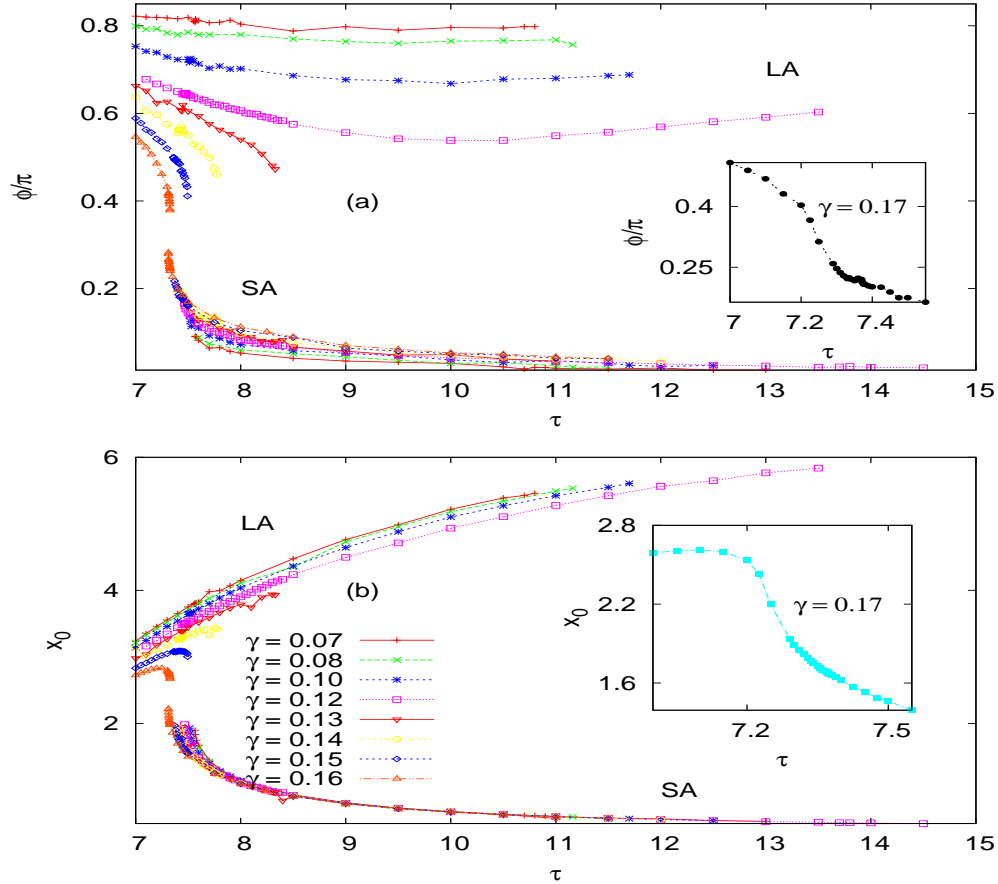


FIG. 4: Plot of the phase lags  $\phi$  (a) and amplitudes  $x_0$  (b) of the trajectories as a function of period  $\tau$  of the drive for various values of  $\gamma$ . We obtain two branches, for each  $\gamma$ , one correspond to SA and the other to LA. For each  $\gamma$  there is a region (the coexistence region) of  $\tau$  where both SA and LA appear but in separate branches. The inset shows that there is only one single continuous branch for  $\gamma = 0.17$ .

Before we proceed to study SR it will be quite appropriate to appreciate the nature of these states SA and LA. These states make their appearance at  $T = 0$  and persist to temperatures  $T$  much smaller than the potential barrier height of maximum 2 and driven by a subthreshold field of amplitude  $F_0 = .2$ . In Fig. 4a we plot the phase lags  $\phi$  between these

states of mean trajectories  $\bar{x}(t) = x_0 \cos(\omega t - \phi)$  and the drive field  $F(t)$  and in Fig. 4b, their amplitudes  $x_0$  are plotted as  $\tau = \frac{2\pi}{\omega}$  is varied. We notice that both  $\phi$  and  $x_0$  change continuously as  $\tau$  is varied for both the states for  $\gamma$  values ranging from .07 to 0.16. The curves for SA and LA are clearly separated. The nature of variation of the curve for LA (SA) is just a continuation even at the boundaries where SA (LA) makes its appearance for the first time. A state, thus, either exists or does not exist at all and not that a state emerges out of the other state as  $\tau$  is varied. It is clearly not a case of bifurcation at the boundary; these states have their independent identities. Bifurcations and associated chaos occur only at large  $F_0$  values[23]. For  $\gamma \geq .17$ , however, we get just one kind of trajectory whose  $\phi$  and  $x_0$  change continuously as  $\tau$  is varied in the entire range (insets of Figs. 4). One cannot identify from the graph to call the trajectories SA or LA for  $\gamma \geq .17$ .

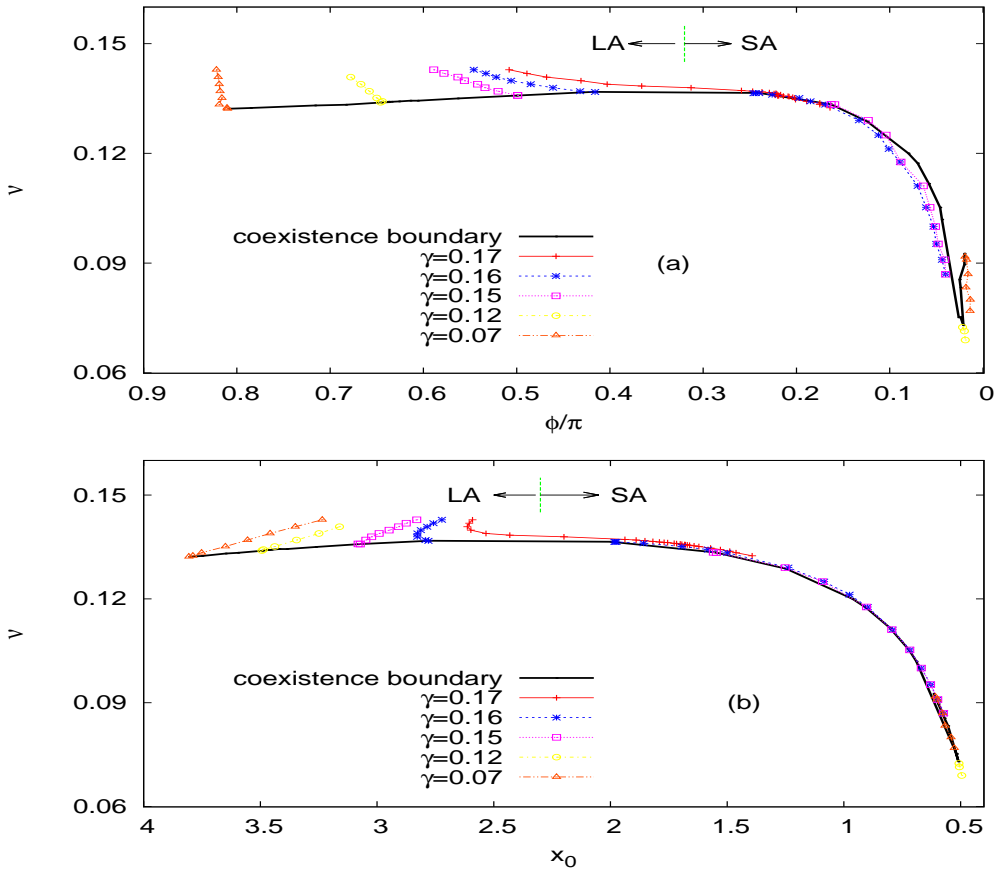


FIG. 5: Replot of Fig.4 of  $\nu(= \frac{1}{\tau})$  versus  $\phi$  (a) and  $\nu$  versus  $x_0$  (b). The thick line shows the boundary of the coexistence region of SA and LA. We have the SA and LA branches outside the coexistence region of various  $\gamma$  values.

In order to gain a little more insight into the dynamical states and their coexistence, the Figs. 4a and 4b are redrawn in Figs. 5a and 5b. In Fig. 5a the frequency ( $\nu = \frac{1}{\tau}$ ) of  $F(t)$  is plotted against  $\phi$  and in 5b the frequency is plotted against the amplitude  $x_0$  of the trajectories  $x(t)$  for various constant  $\gamma$  values. The boundary of the region of coexistence of the two states is shown prominently leaving the region itself blank. The blank bounded region separates the two regions of occurrence of pure LA and SA states. An analogy may be drawn with the liquid-gas pressure-density phase diagram with the isothermals replaced by the constant  $\gamma$  curves of Figs. 5. The SA states ('phases'), of course, run close to the boundary. In the liquid-gas case the mass of the system is conserved whereas in this case the total number of (LA+SA) states remains constant. The curve with  $\gamma = .17$  has a clear analogy with an isotherm above the critical point in the liquid-gas case. However, there are shortcomings too. For instance, a constant  $\gamma$  curve ends at the boundary on the LA side at a different frequency  $\nu$  from the  $\nu$  where the curve emerges out of the boundary on the SA side. Also, the boundary on the SA side has a curious unbounded upturn for all  $\gamma < .12$ . This peculiarity comes about because  $\tau$  decreases along the SA side boundary as  $\gamma$  is reduced from  $\gamma = .12$  in Fig.3. An another computational shortcoming in Fig. 5a is discussed in the last Section of this paper. We are thus justifiably tempted to call the dynamical states to be in the LA and SA phases.

Fig. 6 shows the variation of  $\langle \overline{W} \rangle$  as a function of temperature for  $\gamma = .12$  for a range of values of the period  $\tau$  of the drive field. Though  $\langle \overline{W} \rangle$  shows peaking behaviour in all the graphs, these graphs can be classified into three qualitatively distinct groups. The three groups of  $\tau$  can be identified by a careful look at the insets of Fig. 6. For the group of graphs corresponding to the small  $\tau$  values  $\langle \overline{W} \rangle$  peaks at very small  $T$ . At such small  $T$  only intra-well transitions take place between SA and LA and no inter-well transitions are possible. Thus, as remarked in the introduction, this peaking of  $\langle \overline{W} \rangle$  cannot actually be termed as SR in a periodic potential. On the other hand, the graphs corresponding to the large  $\tau$  values show a broad peak. They peak at temperatures  $T > .5$ . In this case, the peaking temperature is too large for the peak to be considered as a sensible SR. The graphs corresponding to the intermediate  $\tau$  show the nature of typical SR with appreciably large inter-well transitions at the peak of  $\langle \overline{W} \rangle$  and a characteristic initial dip. This dip indicates that SA states are more stable than LA states for these parameter values. A detailed analysis shows that reasonable SR can be obtained in quite a narrow range of  $\tau$

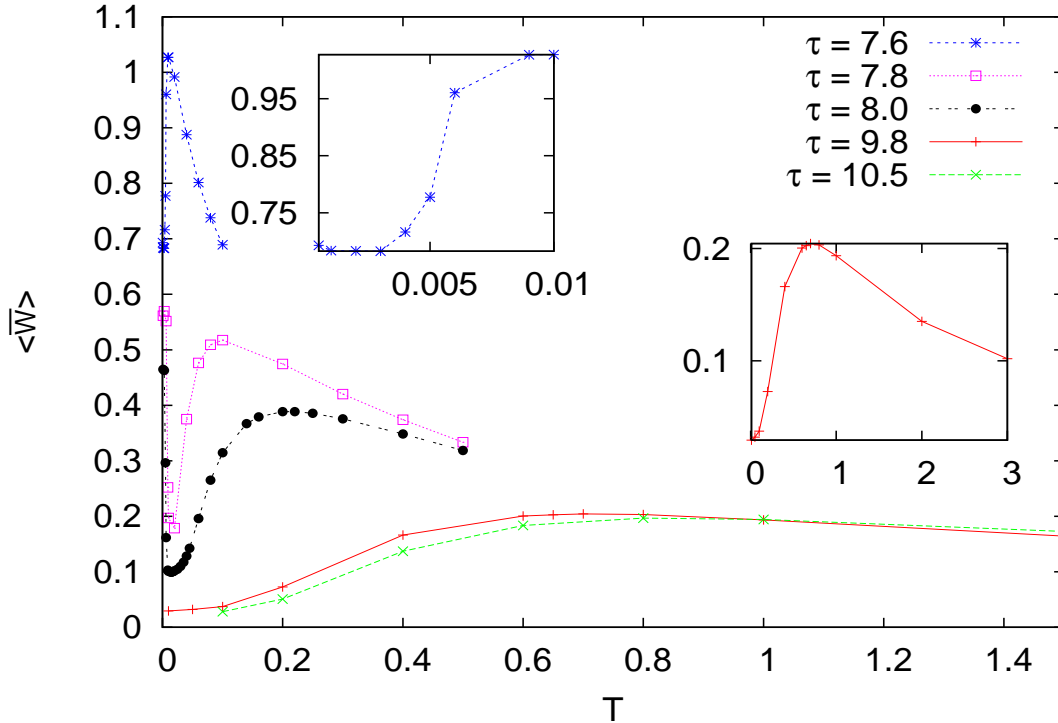


FIG. 6: The input energy  $\langle \overline{W} \rangle$  is plotted as a function of temperature  $T$  for various values of the period  $\tau$  of  $F(t)$ , for  $F_0 = 0.2$  and  $\gamma = 0.12$ . The curves are qualitatively separated into 3 groups corresponding to small, intermediate and large  $\tau$  values. The upper inset shows the variation of  $\langle \overline{W} \rangle$  for smaller  $\tau$ , indicating that there is no appreciable dip at low temperatures. The lower inset is a condensed version of large  $\tau$  curves, showing the  $\langle \overline{W} \rangle$  peaks at large temperature  $T \sim 1.0$ . The intermediate  $\tau$  curves show typical SR behaviour with a characteristic dip at low  $T$ .

where the fraction of SA lies roughly between .3 and .7 at low temperatures. This range lies near about  $\tau = 8$  for almost all values of  $\gamma$  between 0.07 and 0.16, Fig.3.

## B. The biharmonic drive

From the above discussion it follows that physically reasonable SR can be obtained only for values of  $\tau$  around 8, for this is the region where the two dynamical states occur in comparable fractions. We, therefore, consider a biharmonic drive with the main frequency close to  $\omega = 2\pi/8$ . Henceforth, we take the period of the main component of the drive to be 8 unless otherwise stated. Therefore, in the case of biharmonic drive the harmonic component has the period of 4 and that of the subharmonic component a period of 16. Both

these periods are far away from the range of periods where SA and LA occur in comparable fractions. Therefore, neither the harmonic component nor the subharmonic component alone is expected to contribute directly to the occurrence of SR. But their presence in the biharmonic (harmonic and subharmonic) drive case has considerable influence on the occurrence of SR and RE.

The presence of the harmonic component enhances the crest(trough) and distorts the (trough) (crest) of the main component. Nevertheless, the main component ( $\omega \approx \omega_0$ ), being the fundamental component, is always reinforced by the harmonic component. Therefore, one would expect SR to occur almost throughout the range of  $f_m$  except at close to  $f_m = 0$ . The subharmonic component, in this case being the fundamental component, successively enhances and reduces the alternate peaks (troughs) of the main component of  $F(t)$  depending on the phase  $\theta$ . However, appreciable peaks at the period of the main component appears only for large  $f_m > .6$ . Therefore, one does not expect SR to occur at smaller values of  $f_m$ . However, one can expect RE, even if feeble, to occur throughout the range of  $f_m$  except at  $f_m = 0, 1$  for both harmonic and subharmonic drive cases.

Intuitively thinking, the ratchet current  $\bar{v}$  should decrease if dissipation of energy of the system  $\langle \bar{W} \rangle$  increases given a drive field. This is what usually happens at large temperatures where both energy dissipation and ratchet current vary monotonically and  $\bar{v}$  does not show current reversal. However, we are interested in studying the occurrence of both SR and RE simultaneously. We may, therefore, also witness increasing ratchet current with increasing dissipation.

### 1. Harmonic field drive

Consider the external biharmonic field drive of the form given by Eq. (2.11). In the following we take a fixed value of  $\gamma = 0.12$  and the period of the main frequency term  $\tau = 2\pi/\omega = 8$ . In this case the harmonic component enhances the amplitude of the main frequency component. Fig. 1 gives the values of  $\bar{W}$  corresponding to the states LA ( $.17 < F_0 < .226$ ), SA ( $F_0 < .222$ ), LAH3 ( $.217 < F_0 < .222$ ), LAH2 ( $.226 < F_0 < .25$ ) and also when the system shows chaotic behaviour at large  $F_0 > .25$  values. Fig. 7a gives an idea of fractions of the state SA for various values of  $F_0$  for  $f_m = .2$ ,  $T = .000001$ , and  $\theta = 0$ . Fig 7b provides the same information as Fig. 7a but for  $\theta = \pi$ . In these figures no distinction



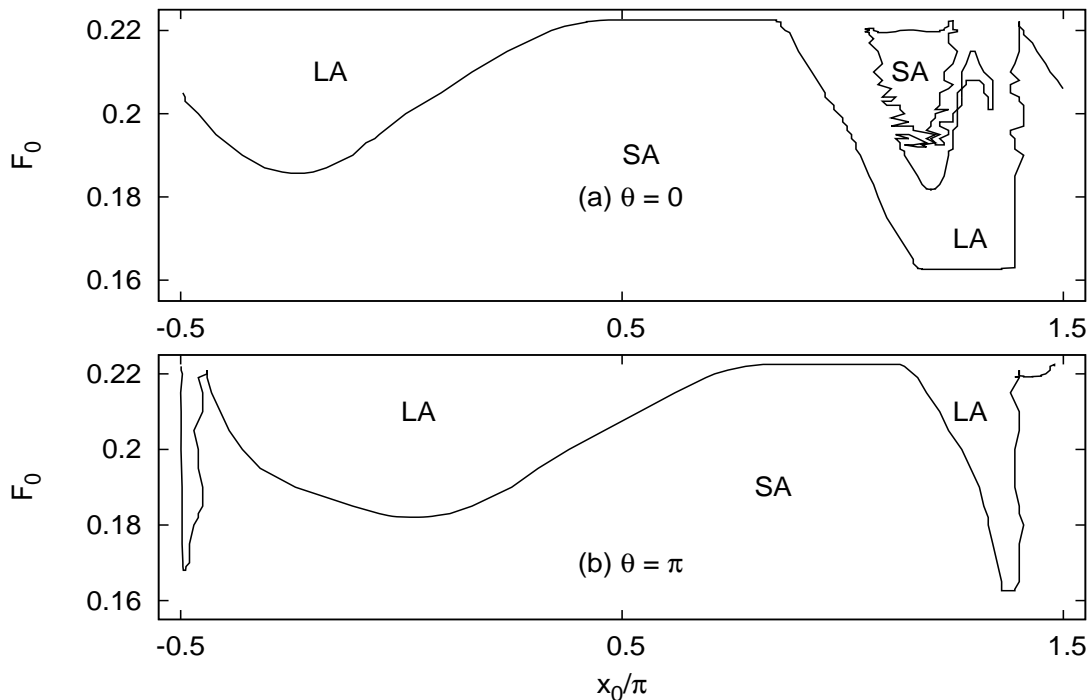


FIG. 7: shows the regions of LA and SA states obtained for initial positions  $x_0/\pi$  lying between  $-0.5$  and  $1.5$ , ie. within a full one period of the potential for the initial phase  $\theta$  of  $F(t)$ ;  $\theta = 0$  (a) and  $\theta = \pi$  (b), for  $f_m = 0.2$  and  $\gamma = 0.12$  at  $T = 0.000001$ , and  $\tau = 8$ .

has been made between LA and LAH3. Fig. 8 also gives the same information as Figs. 7 but also shows how the SA boundary shifts as  $f_m$  is changed for  $\theta = 0$ . The informations provided in the Figs. 1, 7, and 8 are helpful in appreciating the nature of variation of input energy  $\langle \overline{W} \rangle$ . Since, SR does not occur for large  $F_0$  values we restrict our studies to  $F_0 \leq .21$ .

In Fig. 9,  $\langle \overline{W} \rangle$  (a) and the mean velocity  $\overline{v}$  or the ratchet current (b), are plotted as a function of temperature for different values of  $f_m$  and  $F_0 = 0.2$  and  $\theta = 0$ . The occurrence of both SR (Fig. 9a) and RE (Fig. 9b) is evident. However, SR and the maximum of ratchet current  $\overline{v}$  occur at widely separated temperatures (inset of Fig. 9a). Thus, the simultaneous occurrence of SR and RE is beyond dispute, though their connection is not clear. It is to be noted that the effective amplitude  $F'_0$  for  $F_0 = 0.2$  and  $f_m = .2$  of the harmonic drive, Eq.(2.4), is 1.0. The amplitude is just at the threshold value making the potential barrier disappear momentarily every period in one direction whereas the barrier

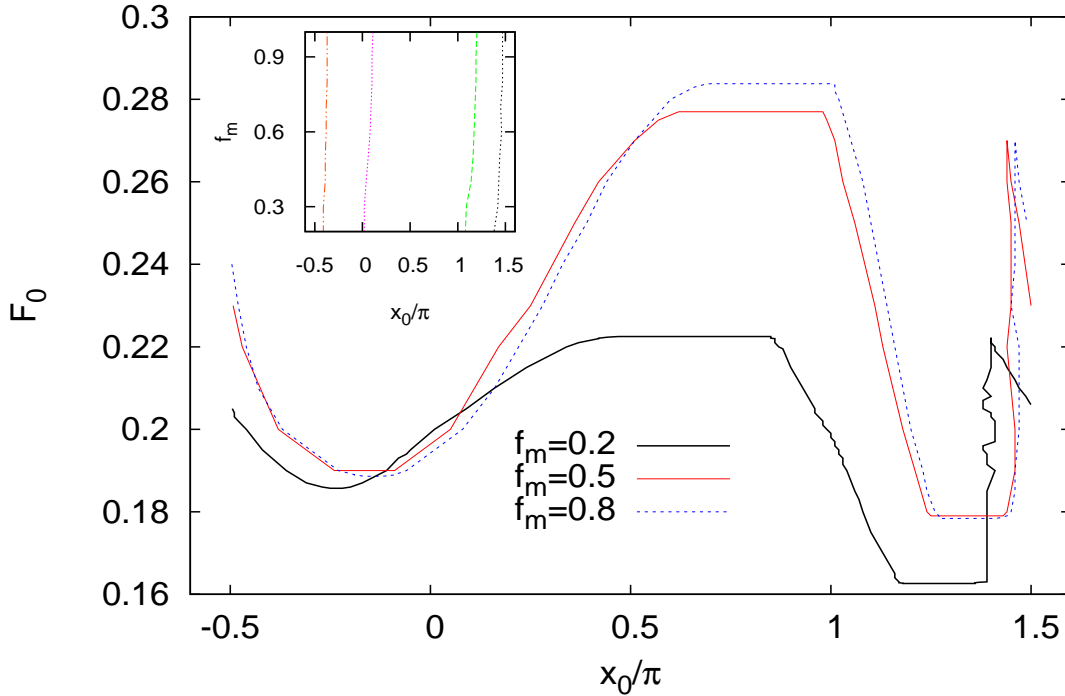


FIG. 8: shows the region of the states LA and SA, as in Fig.7, for three values of  $f_m = 0.2, 0.5$  and  $0.8$ ,  $\tau = 8.0$ ,  $\gamma = 0.12$  at  $T = 0.000001$ . The inset shows how the boundary changes as  $f_m$  is varied for a fixed  $F_0 = 0.2$ .

remains finite in the other direction throughout the period. For  $F_0 = 0.2$  and  $f_m < .2$  the potential barrier disappears for a finite interval of  $t$  in a period whereas for  $F_0 = 0.2$  and  $f_m > .2$  the barrier always remains finite but unequal in the two directions. In either case this favours an asymmetric net particle motion with the assistance of fluctuating forces, but with no net impulse applied, resulting in RE. The presence of the harmonic component of  $F(t)$  induces RE but, as explained earlier, it has only a supporting role to play for the occurrence of SR.

The inset (ii) of Fig. 9b shows that the ratchet current rises fast as the fraction of the main component  $f_m$  of  $F(t)$  is decreased. This is because we have kept the parameter  $F_0$  fixed at  $.2$  for various  $f_m$  values. However, decreasing  $f_m$  corresponds to increasing  $\alpha = \frac{f_h}{f_m}$  which also increases the effective amplitude  $F'_0$  (Eqn. (2.7)) and hence  $\bar{v}$ . The variation is particularly steep for  $f_m < .2$  because  $F'_0 > 1$  and hence the potential barrier disappears for a finite fraction of the period of  $F(t)$  in one direction whereas the barrier remains large in

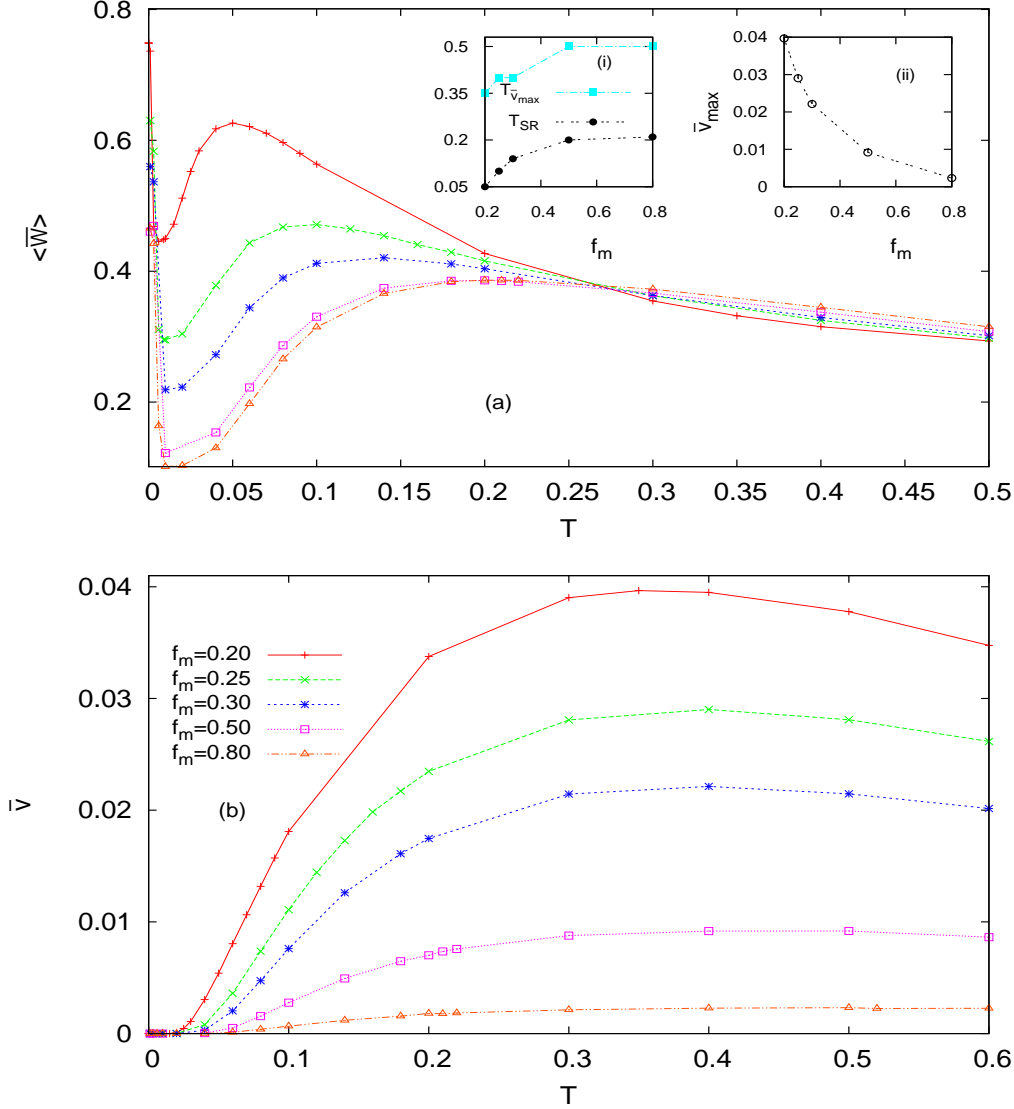


FIG. 9: The curves show the occurrence of SR (a) for  $f_m = 0.2, 0.25, 0.3, 0.5$  and  $0.8$  for  $\tau = 8.0$ ,  $F_0 = 0.2$  and  $\gamma = 0.12$ . Fig. 9(b) shows the variation of the ratchet current  $\bar{v}$  again as a function of temperature  $T$  for the same parameter values. Inset (i) of (a) shows the variation of  $T_{SR}$ , the temperature at which  $\langle \bar{W} \rangle$  peaks, and variation of  $T_{\bar{v}max}$ , where  $\bar{v}$  peaks as a function of  $f_m$  (obtained from (b)). The inset (ii) shows how the peak value of  $\langle \bar{W} \rangle$  vary as  $f_m$  is varied for a fixed value of  $F_0 = 0.2$ .

the other direction. Therefore, a different effect of  $f_m$  will be revealed if  $F'_0$  is kept fixed and  $f_m$  is varied.

Fig. 10 shows the variation of  $\bar{v}$  as a function of  $f_m$  for a fixed value of  $F'_0 = .8$  for  $T = .01$  and  $.2$ . The variation is as it should be because  $f_m = 0$  and  $1$  correspond to pure sinusoidal

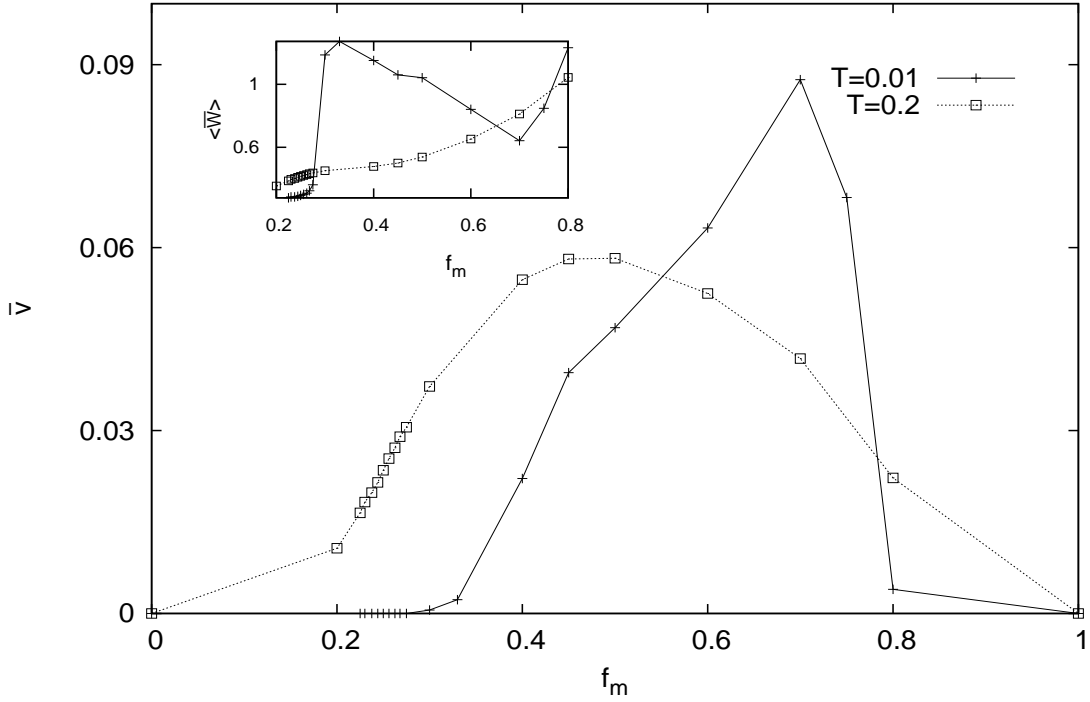


FIG. 10: The variation of  $\bar{v}$  is shown as a function of  $f_m$  for a fixed value of  $F'_0 = \frac{F_0}{f_m} = 0.8$  at temperatures  $T = 0.01$  and  $0.2$ . The inset shows the corresponding variation of  $\langle \bar{W} \rangle$ .

drive and hence there is no asymmetry in the system for a preferred direction, either to the right or to the left, of flow;  $\bar{v}$  must be zero at these two extreme values of  $f_m$  and nonzero at the intermediate values. However, for  $F'_0 = .8$ , SR can be obtained only for a narrow range of  $f_m$  that lies between  $f_m = .2$  and  $.3$  where  $(.17 < F_0 \leq .21)$ . For comparison, we have plotted  $\langle \bar{W} \rangle$ , in the inset, for the same parameter values. Only at large  $f_m$  values  $\langle \bar{W} \rangle$  and  $\bar{v}$  vary such that one increases while the other decreases. But at or near the regions of occurrence of SR dissipation  $\langle \bar{W} \rangle$  and the current  $\bar{v}$  vary in the same way, at least for a part of the range of  $f_m$  values.

In Fig. 11,  $f_m$  is taken equal to  $0.2$  ( $\alpha = 4$ ) and  $\langle \bar{W} \rangle$  (a), and  $\bar{v}$  (b) are plotted for various  $F_0$  values ( $.17, .18, .19, .2$  and  $.21$ ). Note that for  $F_0 \geq .22$  no SR can be obtained. From these figures it is clear that in this range of parameters both SR and RE occur. The inset of Fig. 11a again shows that  $\langle \bar{W} \rangle$  and  $\bar{v}$  peak at widely separated temperatures, that is, they do not vary in total unison with the variation of temperature. Note that as  $f_m$  is increased the effective amplitude  $F'_0$  decreases, correspondingly the inter-well transitions

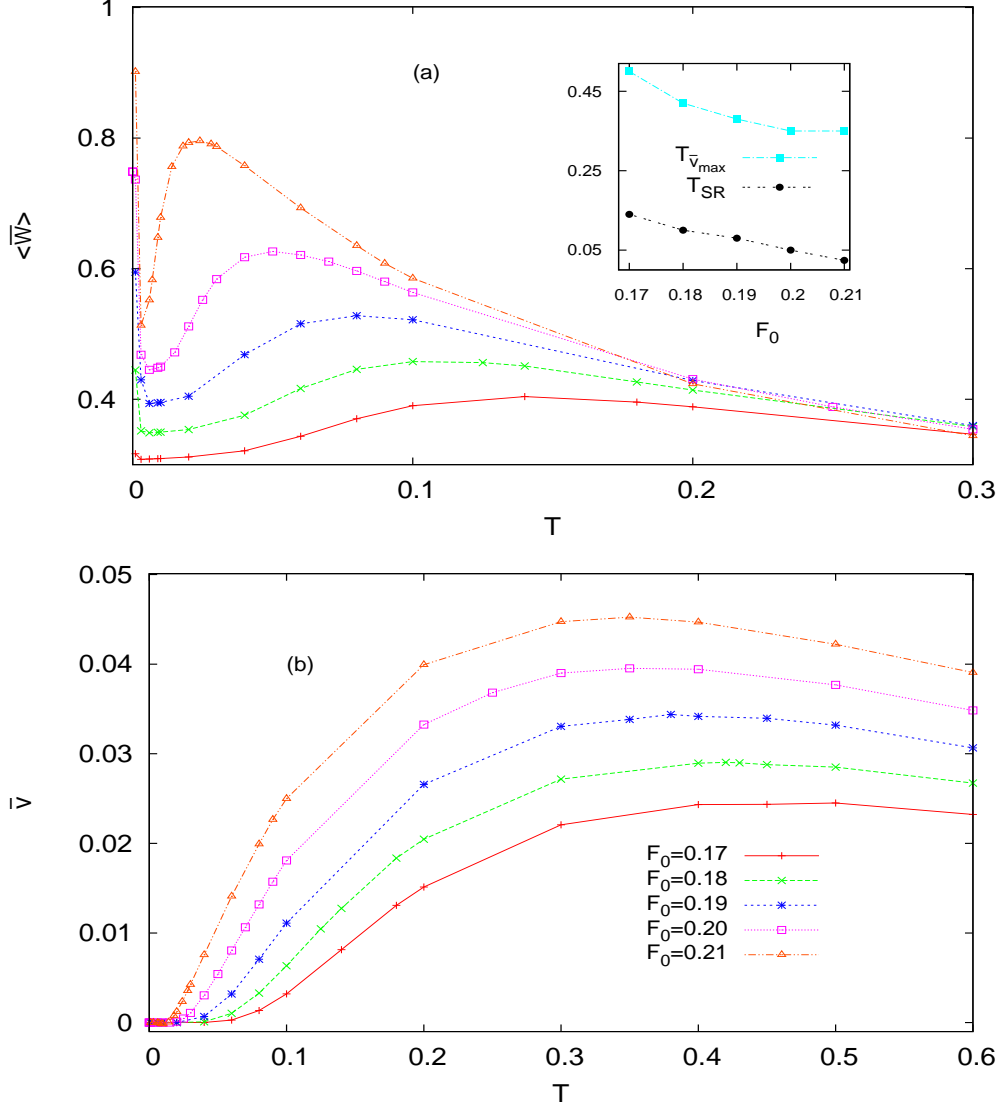


FIG. 11: Same as in Fig.9 (a) and (b) but for various values of  $F_0$  ( $= 0.17, 0.18, 0.19, 0.20$  and  $0.21$ ) where SR occurs, for  $f_m = 0.2, \gamma = 0.12$  and  $\tau = 8.0$ . Again the inset of (a) shows the variation of  $T_{SR}$  and  $T_{\bar{v}_{max}}$  with  $F_0$ .

become less probable and hence  $T_{SR}$  shifts to higher values.

## 2. Subharmonic drive

In this section we consider the subharmonic field drive, Eqn. (2.12). Naturally, it has a period of  $\frac{4\pi}{\omega}$  representing the fundamental frequency of  $F(t)$  instead of  $\frac{2\pi}{\omega}$  as in case of harmonic drive. Yet, we call the term with period  $\tau = \frac{2\pi}{\omega}$  as the main frequency term because

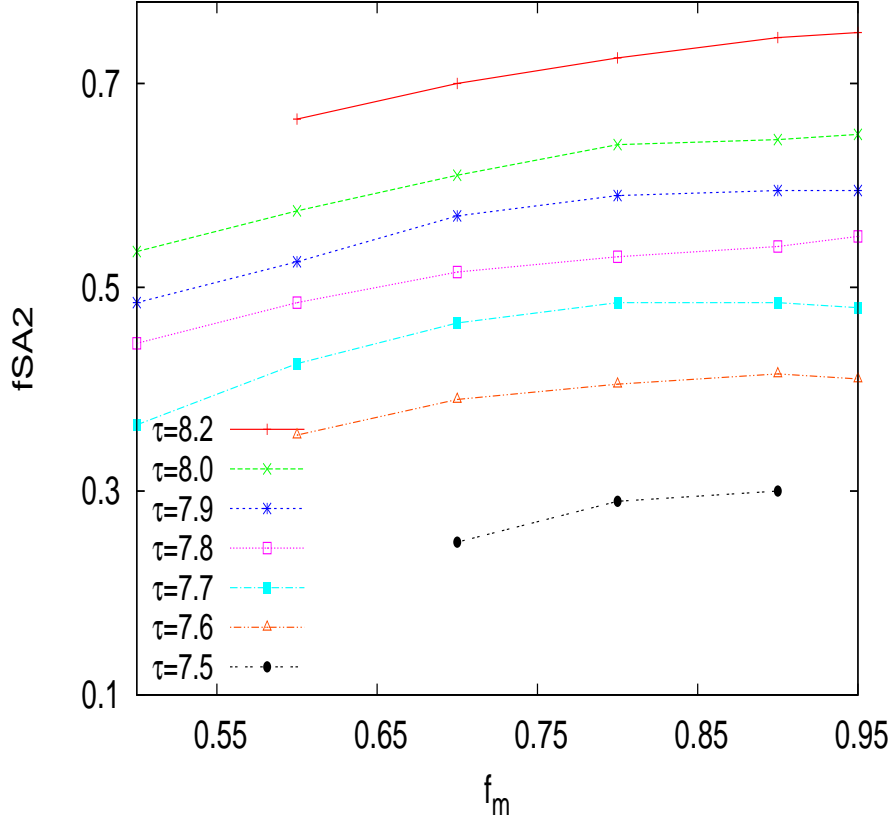


FIG. 12: The figure shows the variation of the fraction,  $f_{SA2}$ , of SA2 state, as  $f_m$  is changed for various values of  $\tau$  and  $F_0 = 0.2, \gamma = 0.12$  in the subharmonic drive case.

we take  $\omega \approx \omega_0$ . As a consequence the particle trajectories obtained have a periodicity of  $2\tau$  corresponding to the fundamental frequency of  $F(t)$ . These trajectories, again, are of two kinds representing the two dynamical states SA2 and LA2 in place of SA and LA, respectively, of the harmonic drive case. Though the period of trajectories corresponding to the states SA2 and LA2 is  $2\tau$ , the main frequency term with period  $\tau$  is responsible for the occurrence of SR. The subharmonic component with frequency  $\frac{\omega}{2}$  of the drive, however, helps in obtaining RE.

We restrict our calculations, in this section, to  $\gamma = 0.12$ . Figure 12 provides a rough guideline for the proper choice of  $\tau$  for various values of  $f_m$  for  $F_0 = .2$ . So far a sort of thumb rule has emerged that the best region in the parameter space where SR can usually be obtained is where the two dynamical states appear roughly in the same ratio (with a tolerance of less than 20 per cent) at low temperatures. The curves at the lower end of  $f_m$

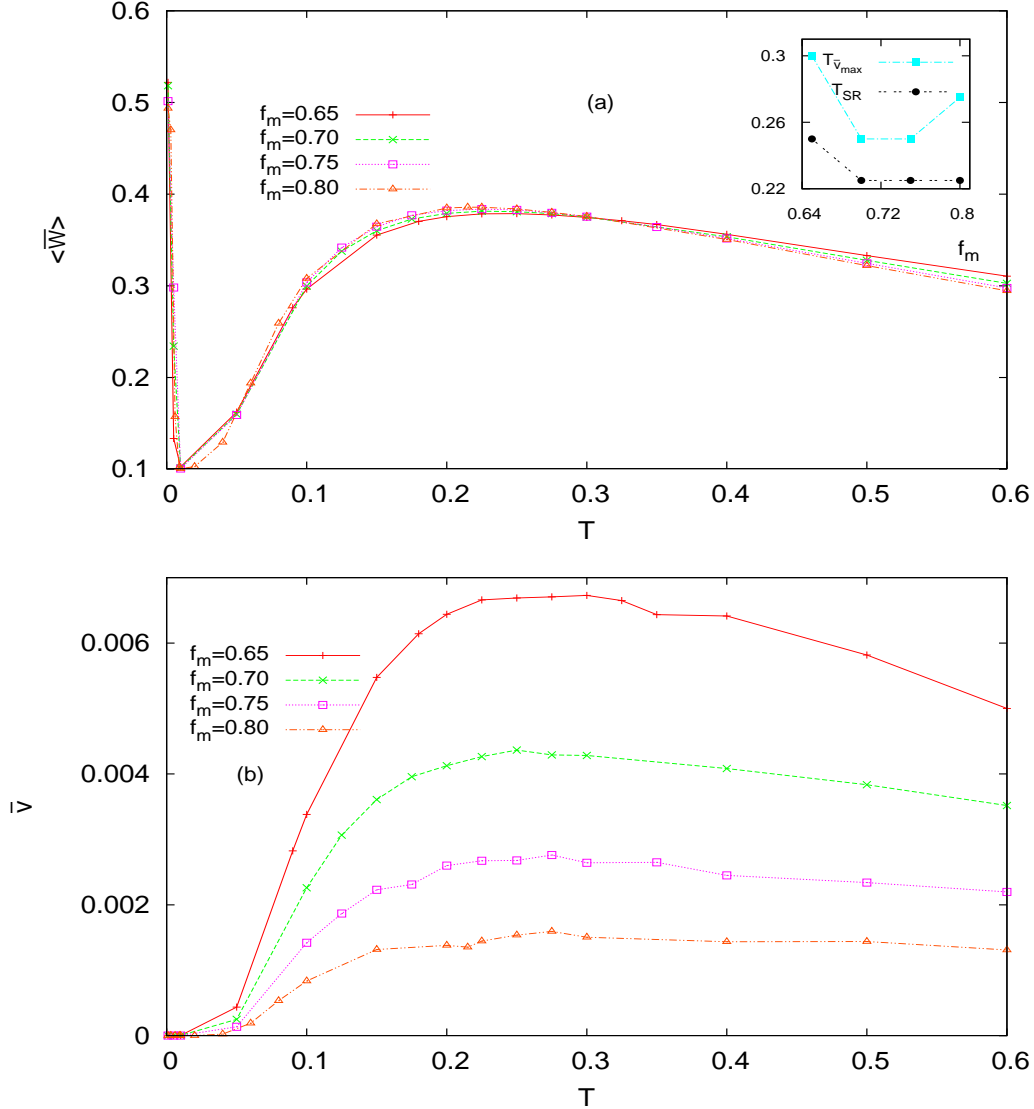


FIG. 13: Just as in Fig.9,  $\langle \overline{W} \rangle$  and  $\overline{v}$  are plotted as a function of  $T$  for various values of  $f_m$  in the subharmonic drive case. The inset of the figure shows the locations ( $T$ ) of the maxima of  $\overline{W}$  and  $\overline{v}$  for  $F_0 = 0.2$ ,  $\gamma = 0.12$  and  $\tau = 8.0$ .

is abruptly ended because one of the dynamical states, namely LA2, disappears for all  $f_m$  less than the edge of  $f_m$  in the graphs.

We explore the occurrence of SR and RE in the region of parameter space where the occurrence of SA2 is around 50 per cent. In Fig. 13, we plot  $\langle \overline{W} \rangle$  (a) and  $\overline{v}$  (b) as a function of temperature  $T$  for  $F_0 = .2$ ,  $\tau = 8$  and  $f_m = .65, .7$ , and  $.8$ . For  $f_m < .65$  no reasonable SR could be obtained though  $\overline{v}$  becomes large. For  $f_m \geq .9$ ,  $\overline{v}$  becomes too small. Interestingly, the inset of Fig. 13a summarizes the result showing that  $\langle \overline{W} \rangle$  and  $\overline{v}$  both

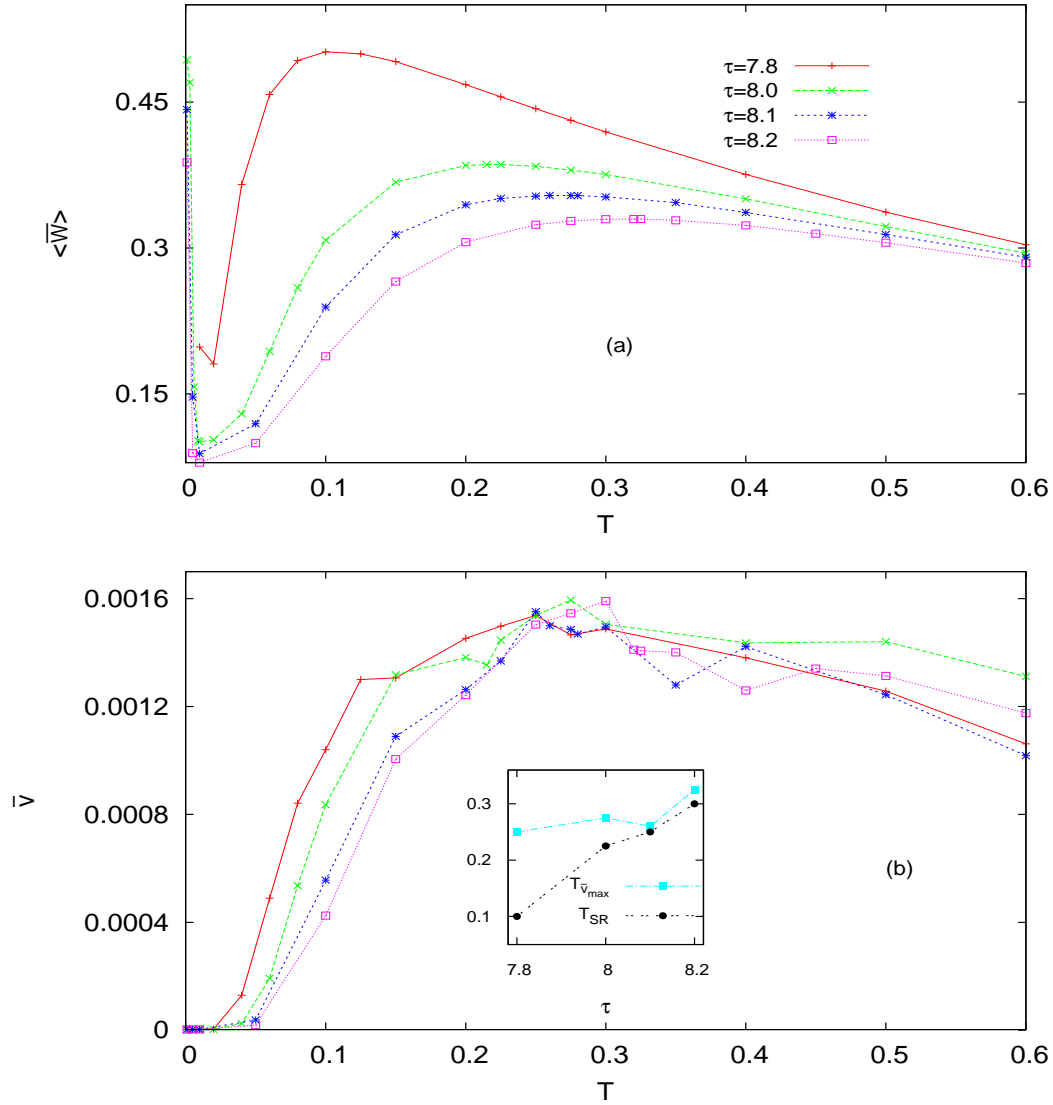


FIG. 14: Same as in Fig. 13 but for various values of  $\tau$  and  $f_m = 0.2, F_0 = 0.2$  and  $\gamma = 0.12$ . The inset of (b) shows the variation of the location of (along  $T$  axis) of the maxima of  $\langle \overline{W} \rangle$  and  $\bar{v}$ .

peak at temperatures lying in a range between .2 and .25, though not exactly at the same temperature.

In Figs. 14a and 14b, respectively, show the variation of  $\langle \overline{W} \rangle$  and  $\bar{v}$  with temperature for  $F_0 = .2, f_m = .8$  and  $\tau = 7.8, 8.0, 8.1$  and  $8.2$ . One can observe that  $\langle \overline{W} \rangle$  peak at temperatures ranging between .1 and .4 whereas  $\bar{v}$  peak in a narrow range lying between .25 and .3. Therefore for a specific  $\tau$  both will peak at the same  $T$  value. However, this will only be a happy coincidence and not a general rule that both show peaking behaviour at the same temperature or in a close range.



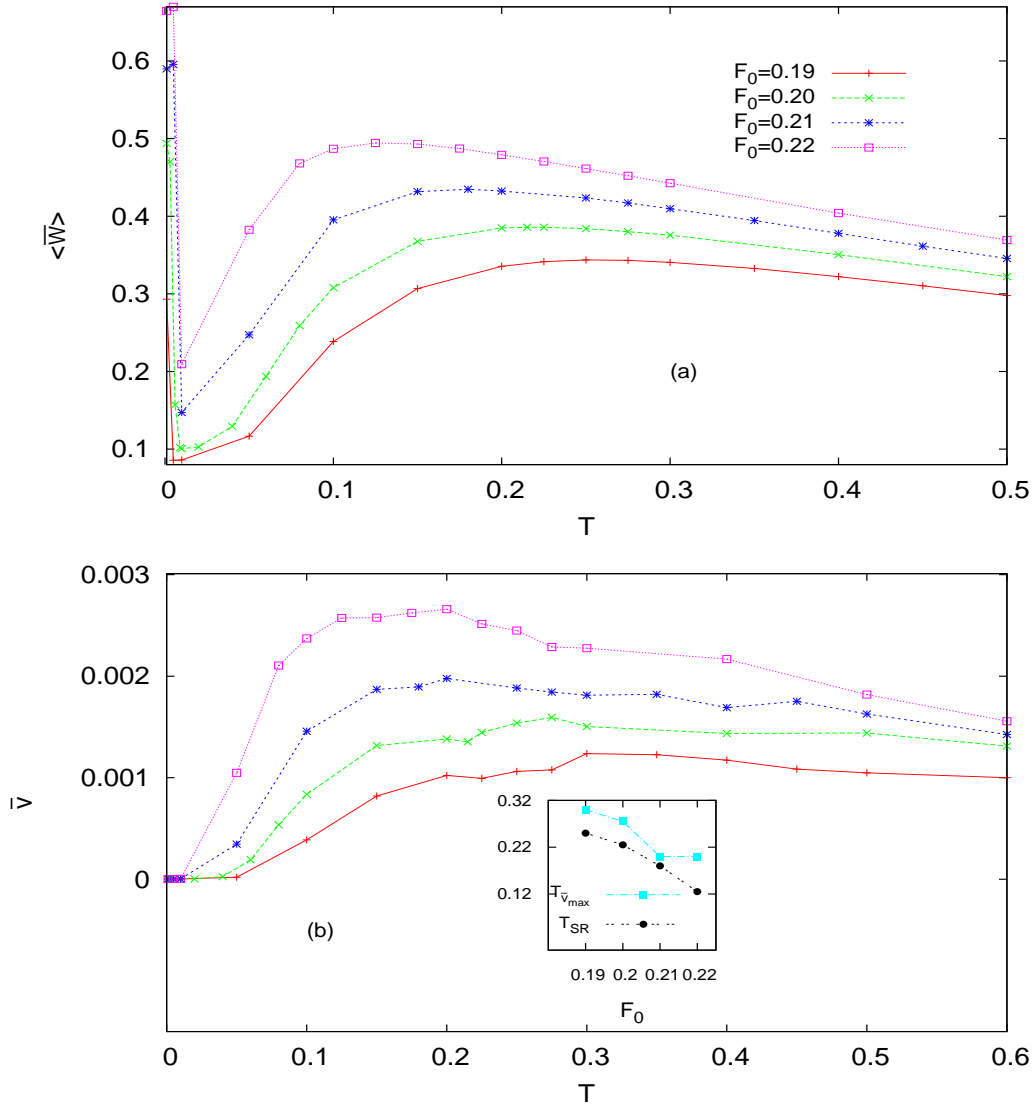


FIG. 15:  $\langle \overline{W} \rangle$  and  $\bar{v}$  are plotted as a function of temperature  $T$  for various values of  $F_0$  and  $f_m = 0.2, \tau = 8.0$  and  $\gamma = 0.12$ . The inset of (b) shows the location of the maxima of  $\langle \overline{W} \rangle$  and  $\bar{v}$  as  $F_0$  is varied in the subharmonic case.

We again plot  $\langle \overline{W} \rangle$  and  $\bar{v}$  as a function of temperature, respectively, in Figs. 15a and 15b for  $f_m = .8, \tau = 8$  but now  $F_0 = .19, .2, .21$  and  $.22$ . The peaks of  $\langle \overline{W} \rangle$  lie between  $T = .25$  and  $.1$ . The peak for  $F_0 = .22$  is larger and sharper occurring at  $T \approx .1$ . We obtain a well defined SR for  $F_0 = .22$ . It is to be noted that for  $F_0 = .22$  there was no SR in case of harmonic drive. The upper  $F_0$  limit for the occurrence of SR is thus extended to a larger value in the subharmonic drive case. The  $\bar{v}$  peaks are very broad for smaller  $F_0$  values. It is very ambiguous to pinpoint the temperature at which  $\bar{v}$  peaks, though there is

a clear indication that the peaks lie between  $T = .4$  and  $.1$ . That is, the peak temperatures of  $\langle \bar{W} \rangle$  and  $\bar{v}$  tend to converge for larger  $F_0$  values towards 0.1. We do not plot the graphs for  $F_0 < .19$  because  $\bar{v}$  show relatively broader (almost flat) peak with much smaller heights.

The results of the calculations show that SR and RE do occur in the same region of parameter space but a strong connection between the two phenomena is not conclusive.

#### IV. DISCUSSION AND CONCLUSION

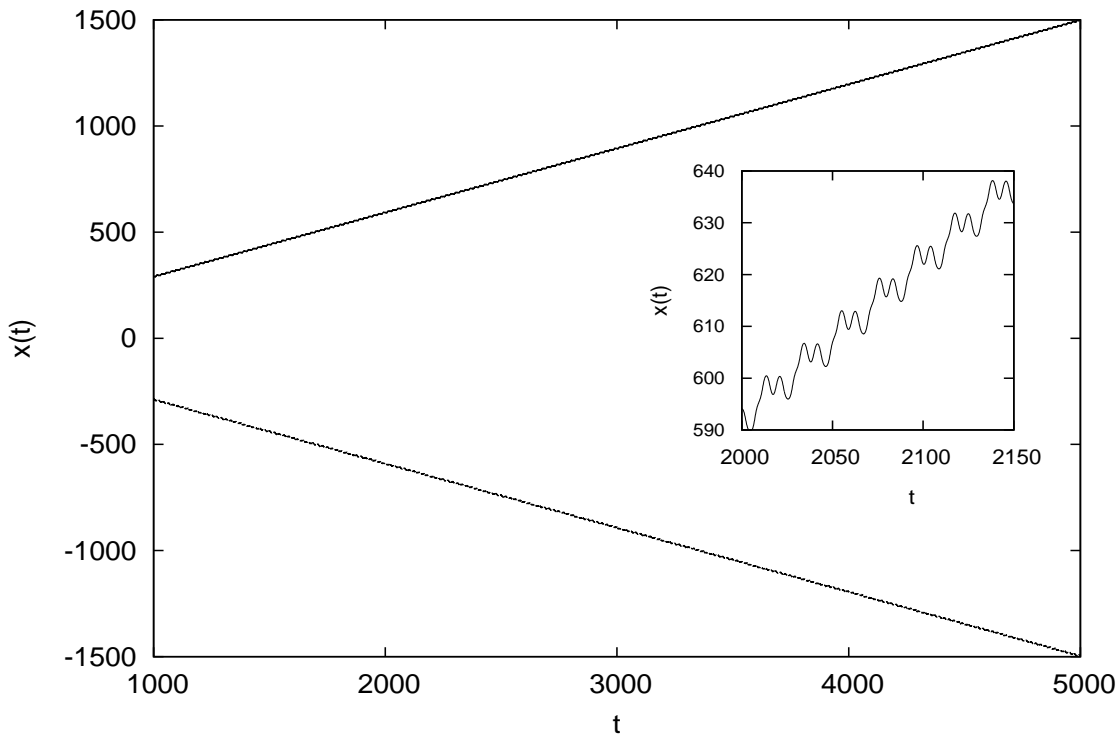


FIG. 16: The figure shows the particle moving forward (for initial condition  $x(0) = -.37\pi$ ) and backward (for  $x(0) = -.36\pi$ ) with the same magnitude of constant average slope for  $\gamma = 0.04$  and  $\tau = 10.4$ . The trajectory is actually periodically jerky as seen from the inset.

The diagram in Fig. 3 closes at around  $\gamma = .17$  indicating that LA and SA do not have separate identity for  $\gamma \geq .17$ . However, the diagram is left open on the lower side of  $\gamma$  at  $\gamma = .07$ . This is partly because of practical difficulty in clearly demarcating the regions of existence of the two states. And partly also because the system's behaviour becomes very complex at low values of  $\gamma$ . For example, for  $\gamma = .04$ ,  $\tau = 10.4$  and some initial  $x(0)$  the

trajectory of the particle becomes constantly (but periodically jerky) forward moving with a constant mean slope, Fig. 16. But for some other  $x(0)$  the trajectory becomes backward moving with the same magnitude of slope. Note that the system is perfectly (right-left) symmetric and therefore these net transport giving trajectories can only be described as strange. However, when the total displacement is averaged over all the initial  $x(0)$  values we get zero mean displacement as it should be for a pure sinusoidal drive.

The states LAH3 and LAH2 shown in Fig. 1 for the biharmonic drive at close to  $T = 0$  are, in fact, unstable against thermal fluctuations. As the temperature is raised from  $T = 0.000001$ , by a small amount transitions takes place from these states to the LA state. This small raise in temperature is much smaller than the typical temperatures where  $\langle \overline{W} \rangle$  peak. Therefore, one can expect  $\langle \overline{W} \rangle$  to peak till  $F_0 \approx .22$  due to the transition of SA to LA (not LAH3). For the small range  $.222 < F_0 < .226$  only LAH3 and LA appear at the lowest temperature. As the temperature is raised LAH3 states quickly go over to LA states giving a small peak of  $\langle \overline{W} \rangle$ . However, this is at a very low temperature where only intra-well thermal transitions are possible. Therefore, no genuine SR occurs in this range of parameter space. For  $F > .225$  the only state LAH2 existing at the lowest temperature also promptly goes over to LA as the temperature is raised by a little. Fig. 1, in fact, indicates that LAH2, as far as the  $\overline{W}$  is concerned, is just a continuation of LA. From this maximum possible value  $\langle \overline{W} \rangle$  can only have a monotonic decrease because the trajectories become chaotic as the temperature is raised further. This can also be inferred from the observation that for a part of the period,  $F(t) > 1$  because the amplitude  $F'_0 > 1$  for all  $F_0 > .2$  and  $f_m = .2$ .

The sharp decrease of energy dissipation  $\overline{W}$  for the chaotic trajectories at large  $F_0$  values appears surprising. However, the decrease can be understood if the trajectories are studied carefully. In the usual situations energy is absorbed from the external field if the particle moves against the force. However, energy absorption becomes negative if particle moves in the direction of the force. In the case of chaotic trajectories the latter situation becomes quite common and hence the decrease of energy absorbed from the field at large values of  $F_0$  and also at large temperatures.

In Fig. 5a, the constant  $\gamma$  curves appear to be intruding into the coexistence region on the SA side. That is only because of our computational inadequacies in pinpointing the coexistence boundary. The LA states disappear gradually and very slowly. Moreover, the

appearance of states (LA or SA) depend very sensitively on the initial condition ( $x(t=0)$ ). We take at most 200 discrete values of the positions within a period of the potential. This cannot be considered as a continuous scanning. There is every possibility of missing an LA state and set the boundary before we have actually reached there (fSA=1.0, for the first time). The  $\gamma = .16$  curve should really be grazing close along the actual boundary. The correspondence with the liquid-gas phase diagram is reasonable.

Finally, to summarise in conclusion, the occurrence of SR in a periodic potential when driven by a biharmonic field of appropriate frequency is shown to be possible. The parameter range in which SR occurs is quite narrow but finite. RE too occurs in this range as it does outside of it. Thus, SR and RE do occur in the same parameter space. However, the peak of  $\langle \overline{W} \rangle$  and the maximum ratchet current occur at temperatures widely separated from each other in the harmonic drive case. In the subharmonic drive case, however, there can be found exceptional circumstances where the maxima of the two quantities may occur at the same temperature. But these are mere coincidences. The occurrence of the two phenomena at the same parameter range can allow for efficient material transport at optimum temperatures at certain frequencies of field drive in periodic potential systems. However, at that optimum temperature particle current need not be a maximum.

Partial financial support from UGC, India under the Special Assistance Program is acknowledged.

- 
- [1] R. Benzi, A. Sutera, and A. Vulpiani *J. Phys. A* 14, L453 (1981).
  - [2] K. Svoboda, C.F. Schmidt, B.J. Schnapp, and S.M. Block, *Nature* 365, 721 (1993); J.T. Finer, R.S. Simmons, and J.A. Spudich, *Nature* 368, 113 (1994).
  - [3] L. Gammaitoni, P. Hänggi, P. Jung, and F. Marchesoni, *Rev. Mod. Phys.* 70, 223 (1998).
  - [4] T. Wellens, V. Shatokhin, and A. Buchleitner, *Rep. Prog. Phys.* 67, 45 (2004).
  - [5] B. McNamara, and K. Wiesenfeld, *Phys. Rev. A* 39, 4854 (1989).
  - [6] S. Fauve, and F. Heslot, *Phys. Lett. A* 97, 5 (1983).
  - [7] B. McNamara, K. Wiesenfeld, and R. Roy, *Phys. Rev. Lett.* 60, 2626 (1988).
  - [8] F. Jülicher, A. Ajdari, and J. Prost, *Rev. Mod. Phys.* 69, 1269 (1996).
  - [9] P. Reimann, *Phys. Rep.* 361, 57 (2002).

- [10] M.C. Mahato, and A.M. Jayannavar, Phys. Lett. A 209, 21 (1995); D.R. Chialvo, and M.M. Millonas, Phys. Lett. A 209, 26 (1995).
- [11] J. Maddox, Nature 369, 181 (1994); *ibid* 369, 271 (1994).
- [12] M.O. Magnasco, Phys. Rev. Lett. 71, 1477 (1993); *ibid* 72, 2656 (1994).
- [13] J. Prost, J. -F. Chauwin, L. Peliti, and A. Ajdari, Phys. Rev. Lett. 72, 2652 (1994); R.D. Astumian, and M.Bier, Phys. Rev. Lett. 72, 1766 (1994).
- [14] J. Rousselet, L. Salome, A. Ajdari, and J. Prost, Nature 370, 446 (1994).
- [15] S. Saikia, A.M. Jayannavar, and M.C. Mahato, Phys. Rev. E 83, 061121 (2011); W.L. Reenbohn, S.S. Pohlong, and M.C. Mahato, Phys. Rev. E 85, 031144 (2012).
- [16] W.L. Reenbohn, and M.C. Mahato, Phys. Rev. E 88, 032143 (2013).
- [17] M. Qian, Y. Wang, and X-J. Zhang, Chin. Phys. Lett. 20, 810 (2003).
- [18] H. Risken, The Fokker-Planck Equation Ch. 11, Springer-Verlag, 1989.
- [19] M.C. Mahato, and S.R. Shenoy, Phys. Rev. E 50, 2503 (1994); T. Iwai, Physica A 300, 350 (2001); M. Evstigneev, P. Reimann, C. Schmitt, and C. Bechinger, J. Phys.: Condens. Matter 17, S3795 (2005).
- [20] E.A. Desloge, Am. J. Phys. 62, 601 (1994).
- [21] R. Mannella, A Gentle Introduction to the Integration of Stochastic Differential Equations. In : *Stochastic Processes in Physics, Chemistry, and Biology*. Edited by J. A. Freund and T. Pöschel, Lecture Notes in Physics, vol. 557, 353. Springer, Berlin, 2000.
- [22] K. Sekimoto, J. Phys. Soc. Jpn. 66, 1234 (1997).
- [23] S. Saikia, Physica A 46, 411 (2014).